Evaluation of micromilling/conventional isotope ratio mass spectrometry and secondary ion mass spectrometry of $\delta^{18}O$ in fish otoliths for sclerochronology

Thomas E. Helser[1], Craig R. Kastelle[1], Jennifer L. McKay[2], Ian J. Orland[3], Reinhard Kozdon[3†], John W. Valley[3]

June 19, 2018

[1] Resource Ecology and Fisheries Management Division, Alaska Fisheries Science Center, National Marine Fisheries Service, National Oceanic and Atmospheric Administration,
7600 Sand Point Way, Seattle, WA 98115, USA
thomas.helser@noaa.gov, craig.kastelle@noaa.gov

[2] College of Earth, Ocean, and Atmospheric Sciences, Oregon State University, Corvallis, OR 97331, USA
mckay@coas.oregonstate.edu

[3] WiscSIMS Laboratory, Department of Geoscience, University of Wisconsin-Madison, 1215 West Dayton Street, Madison, WI 53706, USA
orland@geology.wisc.edu, rkozdon@ldeo.columbia.edu, valley@geology.wisc.edu

[†] Present address: Lamont–Doherty Earth Observatory of Columbia University, 61 Route 9W, Palisades, NY 10964, USA

Corresponding Author: Craig Kastelle, Phone 206 526 4266, Fax 206 526 6723,
craig.kastelle@noaa.gov

27

28 **Running head:** Oxygen isotope measurements in fish otoliths

ABSTRACT

Rationale: Stable oxygen isotope ratios ($\delta^{18}O$) measured in fish otoliths can provide valuable detailed information on fish life history, fish age determination, and ocean thermography. Traditionally, otoliths are sampled by micromilling followed by isotope ratio mass spectrometry (IRMS), but direct analysis by secondary ion mass spectrometry (SIMS) is becoming more common. However, these two methods have not been compared to determine which, if either, is best for fish age validation studies. Hence, the goals were to: 1) determine if the $\delta^{18}O$ signatures from the two different methods are similar, 2) determine which method is best for fish age validation studies, and 3) examine biogeographic and migration history.

Methods: Both analytical techniques, micromilling/IRMS and SIMS, were used to measure $\delta^{18}O$ in six Pacific cod (*Gadus macrocephalus*) otoliths. A series of measurements was made from the center of each otolith to its edge to develop a life-history $\delta^{18}O$ signature for each fish.

Results: The sampling resolution of SIMS analyses was 2-3 times greater than that obtained by micromilling/IRMS. We found an offset between SIMS and micromilling/IRMS $\delta^{18}O$ values, about 0.5‰ on average, with SIMS yielding lower values. However, the $\delta^{18}O$ patterns from both methods (i.e., the number of $\delta^{18}O$ maxima) correspond to the estimated age determined by otolith growth-zone counts, validating fish age determination methods.

Conclusions: Both techniques resolved $\delta^{18}O$ life-history signatures and showed patterns consistent with seasonal variation in temperatures and changes due to fish migration. When otoliths are large micromilling/IRMS can provide adequate resolution for fish age validation. However, SIMS is the better option if greater sampling resolution is required, such as when otoliths are small or specimens are longer lived and have compact growth zones.

Key words

Otolith, Stable oxygen isotopes, Isotope ratio mass spectrometry, Micromilling, Secondary ion mass spectrometry.

1 INTRODUCTION

Oxygen isotope ratios of carbonate structures in marine organisms have been used to derive past temperature and salinity profiles experienced during the lifetime of an organism. The well-established relationship between temperature and $\delta^{18}O$ values have been used in a variety of studies. High-resolution $\delta^{18}O$ measurements of marine coral and shells,[1-5] and fish otoliths[6-11] have proven useful to derive environmental temperature and salinity profiles over an organism's lifetime.[12-13] Grossman and Ku[1] documented the relationship between temperature and $\delta^{18}O$ values in aragonite foraminifera. Fish otoliths have been quite useful in fisheries ecology, in particular, because they are acellular, metabolically inert, and can incorporate chemical properties of water as they grow. As such, otoliths can provide a natural tag, recording biogeographic movements throughout the life of the fish as well as providing a recording mechanism and a way to reconstruct temperature over its life history.[13-15]

In fisheries biology, otoliths have been traditionally used to determine the age of fish and to back-calculate the length at a previous age. Otoliths are calcium carbonate structures found in the inner ear of teleost fish. In most fish, a new layer of calcium carbonate (in the form of aragonite) is deposited over the course of each year forming annual growth zones.[11,16] Annual growth zones, representing one year, are composed of an opaque and a translucent zone representing fast summer and slow winter growth, respectively. The calcium carbonate is deposited onto a protein (otolin) matrix, where the opaque zones have a slightly elevated proportion of protein compared to the translucent zones. The different proportions of protein are thought to be responsible for the occurrence and visibility of different zones within the otoliths.[17-18] Counts of the translucent growth zones are widely used to estimate fish age, although for some species this is difficult and estimated ages need to be independently confirmed or validated.[11,16,18] Otoliths usually develop in isotopic equilibrium

with ambient conditions (sea water temperature and isotope composition), hence, variability in their $\delta^{18}O$ values is generally believed to be inversely related to temperature. [1,11,13] Some fish age studies use environmental signals to determine fish age, which then can be used to validate ages derived from otolith growth band counts. For example, high-resolution sequential microsampling and measurement of $\delta^{18}O$ values in an otolith, from its core, start of life, to margin, end of life, has provided a proxy for annual temperature cycles. A paired maxima and minima in a series of sequential $\delta^{18}O$ values represents a winter and summer respectively, and therefore counting the number of $\delta^{18}O$ maxima is a very accurate tool for determining the age of a fish. Weidman and Millner[6] and Kastelle et al[11] applied this technique to validate the otolith growth zone based ages of Atlantic cod (*Gadus morhua*) and Pacific cod (*Gadus macrocephalus*), respectively, by comparing ages determined from otolith growth zone counts to the number of $\delta^{18}O$ maxima. In this way, the ages determined from otolith growth zone counts, the simpler method, can be validated as accurate when the two methods agree.

There are two methods used to obtain these $\delta^{18}O$ chronological signatures. The first method employs a computer-aided milling instrument, hence forth called micromilling, which mechanically produces powdered aragonite samples by milling a series of tracks parallel to the growth zones and perpendicular to the otolith's direction of growth. The samples are carefully collected and their $^{18}O/^{16}O$ composition is measured (reported as $\delta^{18}O$ values) using conventional acid-digestion followed by isotope ratio mass spectrometry (IRMS). Such mechanical approaches are not without difficulties due to sample mass requirements (>20 μg), small sizes of some otoliths, and the intricacies of acquiring samples at the spatial or temporal resolution needed to detect clear seasonal variation in $\delta^{18}O$ values. The second method, secondary ion mass spectrometry (SIMS, or ion microprobe), has

operationally circumvented many of these problems and greatly increased the sampling resolution of otolith $\delta^{18}O$ chronologies.[9,19] With a 10 μm diameter spot size (1-2 μm deep) it is possible to analyze 100 discrete spots/mm and since most of the volume of a SIMS pit is concentrated near its center, higher resolution is possible with zig-zag sampling. Smaller spots to < 1 μm are also possible but with a trade-off in precision.[20-21] For instance, Matta et al[9] obtained a sample density of up to 50 spot analyses per millimeter and up to 23 samples within a growth year (annulus to annulus) using ion microprobe on a yellowfin sole otolith and Weidel et al[19] analyzed daily growth bands near the core of a bluegill otolith. Concluding that the variation in $\delta^{18}O$ values was a proxy for ambient seawater temperature changes, Matta et al[9] clearly showed a strong seasonal temperature signal and highlighted the use of an ion microprobe for biogeographic and thermal histories. Unlike ion microprobe, however, micromilling systems are within the present ambit of most researchers who study fish behavior and environmental history, and therefore fine-scale resolution ion microprobe may provide a mechanism to confirm the accuracy of the former method. This is particularly true for age validation studies that rely on a greater number of assumptions when sampling at lower spatial resolution. In an effort to determine the practical and operational use of micromilling/IRMS specifically for age validation studies, we measured the $\delta^{18}O$ composition in transects across Pacific cod otoliths using both micromilling/IRMS and ion microprobe. Our goals were three-fold: 1) determine if the $\delta^{18}O$ signatures derived from the two different sampling and mass spectrometry techniques are similar, 2) determine which method is best or necessary for fish age validation studies, and 3) examine biogeographic history on the depth and migration history.

2 EXPERIMENTAL

2.1 Selection and preparation of otoliths

The Pacific cod otoliths utilized in this study were from specimens recaptured during a tagging study conducted by the Resource Assessment and Conservation Engineering Division at the Alaska Fisheries Science Center (AFSC).[22-23] The archival tags used in this study recorded temperature and pressure (depth) approximately every 15 minutes with an accuracy of ± 0.3 °C and approximately ± 3 m, respectively. In this tagging study, 653 adult Pacific cod were released between November 2001 and May 2002 near Kodiak Island in the Gulf of Alaska and near Unimak Island in the eastern Bering Sea, from which 286 were recovered. From the recaptured specimens we chose 6, based first on the longest time at liberty and second, when the times at liberty were similar, those fish with the shortest length at tagging (Fig. 1). Using small fish meant they were likely young; thus, we avoided sampling (described later) from the narrow outer growth zones expected in mature fish. The chosen specimens were 54-67 cm in length at tagging, with at-liberty periods ranging from 268 to 357 days (Table 1).

Both methods of otolith $\delta^{18}O$ analysis require mounted thin sections. The sagittal otoliths from the selected Pacific cod were extracted, cleaned of any membrane or organic material, and stored in 70% ethanol. It was expected that the ethanol storage medium did not alter the $\delta^{18}O$ values of the aragonite.[24] After approximately 8 years of storage, one otolith from each specimen was retrieved, cleaned in a sonic cleaner with 18 Milli-Q® water (Millipore Corp., Billerica, MA, USA), and air dried. Next, the otoliths were embedded in polyester resin, and using an IsoMet™ 5000 linear precision saw (Buehler Ltd., Lake Bluff, IL, USA) two transverse thin sections aligned on the otolith's primordium were extracted for mounting. The thin sections and surrounding resin were mounted on glass microscope slides with Loctite 349 (Henkel Corp.) and polished with silicon carbide wet and dry sandpaper

(using a sequence of 600, 800, 1200 grit) on an EcoMet™ (Buehler Ltd.) grinder. After the mechanical polishing, the thin sections were polished by hand with 0.05 μm MasterPrep® polishing suspension (Buehler Ltd.). This procedure produced thin sections approximately 0.8 mm thick. Digital images were taken of each thin section and the ages were determined by counting the presumed annual translucent zones. At the AFSC, Pacific cod ages (counts of translucent zones) are determined using the otolith break and bake method of which full details can be found in Johnston and Anderl[25] and Kastelle et al.[11]

2.2 Otolith microsampling and dual-inlet isotope ratio mass spectrometry (IRMS)

Microsampling of the thin sections was performed with a specialized micromill designed for sampling small objects such as otoliths. One thin section from each specimen was used for Microsampling. This was the same equipment, a Carpenter Systems CM-2 micromilling system, used in Kastelle et al[11], but some of the procedures differed and are detailed below. The micromill was comprised of a dental drill with a 0.3 mm bit fixed over an X-Y-Z sample stage, stereo microscope, and a high-resolution digital camera. All components of the micromilling system were interfaced and controlled by a computer and software specifically designed for this purpose. The computer guided the stage such that the sample was milled in parallel tracks specified by the operator for each specimen (Fig. 2). The milled region (i.e., the direction or transect) in each thin section was chosen for clarity and differentiation of opaque and translucent zones (Fig. 2). The initial milling was a trough 0.3 mm wide made on the proximal side of the otolith's primordium; the material produced in this initial milling was not used. Each successive milling track shaved a very narrow region off the distal, leading, side of the trough. In this way, the next track (i.e. the first sample) was the otolith's primordium, and the successive tracks progressed distally toward the outer edge of the otolith. Each track shaved a region 30 to 130 μm

174 wide, up to about 1200 um long, and about 200 μm deep, which followed parallel to growth
175 zones reproducing their exact curvature (Fig. 2). The width of each milled track was measured in
176 the center of its length. Each milled track produced approximately 30 to 60 μg of aragonite
177 powder; the actual amount generated depended on the length and width of the track. This
178 procedure allowed 4 to 12 tracks in any one posited year's growth (paired opaque and translucent
179 zones) depending upon the distance between adjacent growth zones. The goal was to have the
180 best possible spatial resolution in the sampling (i.e., as many tracks as possible), and still
181 generate an adequate sample mass of > 25 μg. The powder generated by milling each
182 individual track was collected by hand using microspatulas and the microscope, and was
183 placed in stainless steel sample holders for shipping to the stable isotope laboratory in the
184 College of Earth, Ocean, and Atmospheric Sciences (CEOAS) at Oregon State University.
185 To avoid cross contamination, the thin sections and bit were cleaned with compressed air and
186 a 3 mm wide stiff brush between each sample milling and collection to remove any
187 particulates or powder. The thin sections and bit were also visually inspected with the
188 microscope between each sample milling to confirm a lack of cross contamination.

189 The powdered otolith material generated in the milling procedure was analyzed using the
190 same mass spectrometer procedures as described by Kastelle et al.[11] The details can be
191 summarized as follows. To determine the oxygen isotopic composition, each sample was
192 reacted with 105% orthophosphoric acid at 70 °C using a Kiel III carbonate preparation
193 system (Thermo Scientific) connected to a MAT 252™ dual-inlet isotope ratio mass
194 spectrometer (Thermo Scientific). The aragonite was not pretreated to remove organic carbon;
195 any contribution from the otolith's protein matrix should be minimal because protein does not
196 produce CO_2 when reacted with the acid. Repeat measurements of two isotopic standards, an
197 international calcite standard, NBS-19 (U.S. Geological Survey), and an in-house laboratory

198 calcite standard, Wiley (calibrated with international standards NBS-18 and NBS-19), were
199 made before and after the otolith samples. These standards were used to calibrate the
200 instrument reference gas on a daily basis and estimate standard deviations and 95%
201 confidence intervals. Finally, otolith oxygen isotopic data were corrected using an acid
202 fractionation factor of 1.0090898, which was calculated using the temperature equation of
203 Kim et al.[26] The results are reported in the standard delta notation ($\delta^{18}O‰$) relative to Vienna
204 Pee Dee Belemnite (VPDB). The accuracy of the IRMS relative to NBS-19 was evaluated by
205 comparing the known value, $\delta^{18}O$ = -2.20‰ VPDB, to the averaged measured value, $\delta^{18}O$ =
206 -2.19‰ VPDB, n = 25.

207 **2.3 Ion microprobe and secondary ion mass spectrometry**

208 The same thin sections used for micromilling/IRMS were analyzed with the ion
209 microprobe. The milled thin sections were coarsely re-polished to remove the milled area and
210 produce a new surface, at a level below what was the milled region. The resulting thin
211 sections were about 0.3 to 0.4 mm thick. Next, they were cut from the slides and cast in
212 epoxy disks (exposed on one surface of the disk), 2.5 cm diameter x 4 mm thick, along with
213 small crystals of a calcite standard, UWC-3.[20] The disks and thin sections were finely
214 polished using the same method described previously. Next, they were cleaned with ethanol
215 and deionized water in a sonic cleaner after which they were dried in a vacuum oven at 40 °C
216 for 2.5 hours. Prior to sampling with the ion microprobe, the epoxy plugs and polished thin
217 sections were sputter-coated with ~ 60 nm of gold.

218 *In situ* oxygen isotope ratios were obtained using a CAMECA IMS 1280 large radius,
219 multi-collector ion microprobe at the WiscSIMS Laboratory, University of Wisconsin-
220 Madison. For ion microprobe analysis, transects of sampling spots were chosen to avoid

221 cracks and inclusions, but were strategically placed to coincide with the previously micro-
222 milled distal region of the otolith. Transects, perpendicular to the axis of growth lamina,
223 spanned the cross section of the otolith from the core to the margin (life-history transect).
224 The goal was to obtain 60 – 90 spot samples in the region previously micromilled for
225 comparison between the two methods. However, Pacific cod otoliths do not accrete material
226 simultaneously in all directions, as if they were spheres. After the third or fourth translucent
227 zone, there is variability in the location of active deposition, and in any one axis growth can
228 start and/or stop.[25] As such, the most recent growth in these otoliths from adult fish may only
229 be in one reduced area of the dorsal and ventral axes. Therefore, where feasible, a second
230 shorter transect of ion microprobe spots was placed in the ventral region as a continuation of
231 the longer life-history transect that started in the core (Fig. 2).

232 The ion microprobe settings for this study were the same as used by Matta et al.[9]
233 They sampled otoliths from yellowfin sole (*Limanda aspera*), which are similar in
234 composition to the Pacific cod otoliths we analyzed here. The key instrument parameters are
235 summarized in the following description, and more detail can be found in Matta et al.[9] A
236 primary beam of $^{133}Cs^{+}$ was focused to a spot diameter of ~10 μm on the sample. The
237 analysis of each spot took 4 minutes and resulted in a pit ~1 μm deep (weight ~ 1 ng).
238 Secondary oxygen ions were analyzed in the mass spectrometer set up for high secondary-ion
239 transmission.[27] Groups of 10 to 15 sample spots were bracketed, before and after, by 4
240 analyses of the calcite standard UWC-3 ($\delta^{18}O$ = 12.49‰ Vienna Standard Mean Ocean
241 Water (VSMOW)).[20] Analyses of the bracketing standard were used to calculate the
242 precision (2 s.d.) of sample analyses and to determine the instrumental mass fractionation
243 used to calibrate $\delta^{18}O$ values to the VPDB scale.[9,20,21,27,28] After ion microprobe analysis, we
244 imaged each transect of spots with scanning electron microscopy (S3400-VP-SEM, Hitachi,

Ltd.) to be sure that the spots did not include irregularities or contaminants. Data acquired by ion microprobe, as well as IRMS of micromilled powders, are reported in $\delta^{18}O$ (‰, VPDB) with 2 s.d. precision.

It is difficult to assess the accuracy of our ion microprobe data by comparison to IRMS. This is because different material is sampled by each technique. When measuring the non-homogeneous matrix of a biogenic carbonate at high resolution by ion microprobe, protein or hydrous components contribute to the result. These components are excluded from IRMS analysis during acid digestion of the carbonate. Conversely, sample imperfections can be side-stepped by the ion microprobe, while diagenetic alteration or cracks with contaminants are harder to avoid when micromilling. For ion microprobe analysis of $\delta^{18}O$ in crystalline samples, a homogeneous crystalline ion microprobe standard of similar chemistry (i.e., UWC-3) is ideal for accurate calibration to an isotope scale. It follows that the calibration of biocarbonate analyses by SIMS could be improved by using a matrix-matched biocarbonate standard with homogeneous $\delta^{18}O$. Although we do not presently know of such a biocarbonate standard, efforts to identify one are underway.

2.4 Data analysis

Our goal was to compare the two methods of measuring $\delta^{18}O$, micromilling/IRMS and ion microprobe. Life-history transects within each specimen, from each method, were compared graphically with the following procedure. The $\delta^{18}O$ results were organized and plotted such that values on the independent axis (i.e., x-axis) were the (counts of) $\delta^{18}O$ peaks, from the core (peak number 0) to the margin of the thin section. Hence, the peaks in the data from both methods were matched and lined up, and the $\delta^{18}O$ values between each peak were spaced evenly by manual scaling. The short ion microprobe transects in the region of the

ventral tip are represented by a disconnected section of $\delta^{18}O$ results, usually after the 4th peak (Fig. 3). Subjectivity in determining the location of peaks in the time series was avoided by considering the 95% confidence intervals in the $\delta^{18}O$ results, and the number of data points in a peak or valley.[11] Next, the results in each life-history time series were divided into three sections, and average values were calculated for each section. The first section was from peak 0 to peak 1, the second section was from peak 1 to peak 2, and the third section was the remaining data in the life-history transect. This step provided up to 18 possible pairs of averaged $\delta^{18}O$ values for comparison, and were evaluated using linear regression methods. We expected the slope of the line to be equal to 1.0 while the intercept of the regression would provide a measure of potential offset between approaches.

3 RESULTS

Pacific cod in this study ranged between 5 and 6 years of age based on annual growth zone counts (Table 1). The growth laminae are evident in transverse thin sections, seen in specimen 812 (Fig. 2), as alternating pairs of translucent/opaque zones under reflected light. The untrained eye may incorrectly interpret more growth laminae as annual zones, however examination of otoliths independently by two skilled age reading analysts corroborated an age of 6 years old. Baring one specimen (693), both the ion microprobe and micromilling methods sampled equal numbers of annual growth zones within the common distal region of the otoliths as identified by visual inspection under a stereo microscope. This was by design since we wanted to characterize the $\delta^{18}O$ variability between the two sampling approaches in the same region, over the entire life-history transect, and within individual growth zones. In total we made 452 and 235 analyses of $\delta^{18}O$ with the ion microprobe and micromilling/IRMS, respectively. For more detailed results see data presented in supplemental materials.

292 In general, the transect lengths were comparable for both sampling techniques within
293 each sample over the transverse plane of the thin section from otolith core to margin.
294 Transect lengths for ion microprobe varied between 1.44 mm and 2.82 mm, with between 52
295 and 90 analyses (Table 1). The 10 μm ion microprobe spots had a minimum distance of 5 μm
296 between analyses. The total length micromilled in specimens in the same transverse distal
297 region ranged between 1.64 mm and 2.47 mm, however, the number of milled $\delta^{18}O$ samples
298 achieved ranged between 33 and 44 analyses. Near the margin of the thin section, the typical
299 width of each micromilled track was about 37 μm. The lengths of the micromilled tracks
300 averaged approximately 1000 μm; this provided a typical target sample mass of ~30 μg.
301 Hence, the ion microprobe provided on average a sample rate 2 to 3 times greater than
302 micromilling/IRMS (Table 1). This is illustrated in specimen 812 (Fig. 2) where the sample
303 density was 62.6 samples per mm for ion microprobe, compared to 23.1 per mm for
304 micromilling/IRMS. Furthermore, the spatial resolution of milled samples will be degraded if
305 trenches cross time boundaries or intersect younger material at depth.

306 In all but one specimen, the average $\delta^{18}O$ value measured over the entire life-history
307 transect by ion microprobe was lower than the average obtained from micromilling/IRMS
308 (Table 1; Fig. 3). In all specimens, average $\delta^{18}O$ value from the ion microprobe was near or
309 below a value of 0‰ VPDB, while those for micromilling/IRMS were above 0‰ VPDB.
310 Over all six specimens, the average offset is 0.53‰ (Table 1). Results from both methods
311 show a strong cyclical pattern of $\delta^{18}O$ values across the life-history transects (Fig. 3). Within
312 the cyclical pattern of the time series, a majority of the micromilling/IRMS $\delta^{18}O$ values were
313 near or above the ion microprobe $\delta^{18}O$ values. However, at the $\delta^{18}O$ peaks the two methods
314 were more similar and often overlap (Fig. 3). This pattern in values of $\delta^{18}O$ (IRMS-SIMS) is
315 pronounced near the otolith core (interval between 0 and peak 1 or 2). For example, in

316 specimen 812 the value of ion microprobe $\delta^{18}O$ starts near -3.0‰ VPDB while the
317 micromilling/IRMS $\delta^{18}O$ values start near 0.5‰ VPDB, but at the first peak they are similar.
318 A coherence in the sequence $\delta^{18}O$ values between the sampling approaches, both in terms of
319 the number and the relative position of the peaks and troughs, suggest that both methods of
320 measuring $\delta^{18}O$ in fish otoliths reveal comparable information about fish age and
321 thermography. However, the high-resolution sampling provided by ion microprobe yields
322 much more intra- and inter-annual detail in relative $\delta^{18}O$ values compared to
323 micromilling/IRMS, which is particularly evident in specimens 812, 426 and 778 (Fig. 3).

324 The comparison of average ion microprobe and micromilling/IRMS $\delta^{18}O$ values in
325 each of three sections of the time sequences yielded a significant relationship. A linear
326 regression of IRMS versus ion microprobe $\delta^{18}O$ values was statistically significant (r^2=0.58,
327 p<0.01; Fig. 4). IRMS $\delta^{18}O$ values were linearly dependent on ion microprobe $\delta^{18}O$ values
328 with a slope of 0.477 and intercept of 0.482.

329 **4 DISCUSSION**

330 The relationship between temperature and $\delta^{18}O$ variation in fish otoliths is well
331 established in the ecological literature,[6,14,29] and more specifically for Pacific cod and
332 yellowfin sole in the Bering Sea and Gulf of Alaska.[9-11] Applying this understanding to the
333 current study of patterns of $\delta^{18}O$ variation in Pacific cod otoliths suggests evidence of
334 thermal habitat change over the life of 5- to 6-year-old Pacific cod, as well as seasonal
335 variation in the temperature experienced by fish. High-resolution sampling for $\delta^{18}O$ values in
336 fish otoliths provided a unique perspective on Pacific cod biogeography and migratory
337 behavior, showing both annual cycles and habitat preference for warmer nearshore water
338 during early life stages followed by migration to cooler deeper water. First year juvenile

339 Pacific cod (age 0 years) have been documented to exhibit associations with shallow,
340 nearshore, and coastal areas in the Gulf of Alaska.[30-31] As the juveniles grow they move
341 gradually to offshore cooler coastal water as sub-adults and adults.[32] These movement
342 patterns are confirmed by population level research survey data which shows the greatest
343 concentration of juvenile Pacific cod are in shallower, warmer shelf water until 4 years
344 old.[23,33] During the transition to maturity, between ages 4-5 years,[34] there is a tendency for
345 animals to move toward deeper cooler waters of the continental shelf where they find suitable
346 habitat for spawning.

347 The potential advantage offered by the IMS 1280 ion microprobe over micromilling
348 and conventional IRMS is increased spatial resolution (sample diameter = 10 μm with depth
349 of ~1 μm). This allows for finer temporal resolution of measurements while maintaining high
350 accuracy and precision.[21,27] The methods in this comparative study allowed for a 2-3 times
351 greater temporal sampling density with ion microprobe over micromilling/IRMS. In theory,
352 the ion microprobe spatial resolution in the life-history transects could be greater than this,
353 up to about 200 spots per mm.[35] The otolith thin sections encompass three dimensions, not
354 only *x*- and *y*- planes, but also in depth, the *z*- plane. The micromilled samples were ~200 μm
355 deep (i.e., in the *z*- plane), and we note that the deposition of growth zones may not be
356 orthogonal to the thin section's surface. Hence, because the shaved leading edge of the
357 sampling trough progressed orthogonally to the surface, the sampled material may represent
358 a mechanical averaging over space and time in the otolith; this is especially true when the
359 growth zones are more compact, after about the fourth translucent zone from the core. The
360 ion microprobe analyses are much shallower/smaller (i.e., a spot vs. a track) so they are less
361 likely to integrate unintended time intervals. However, the high-resolution ion microprobe
362 results confirmed that micromilling/IRMS can provide sampling resolution capable of

363 capturing the effect of the seasonal temperatures on otolith $\delta^{18}O$ variation in comparatively
364 short-lived species, relatively large otoliths, or when considering only the first 3 or 4 years.
365 Pacific cod are a good example where some of these situations apply. With fish otoliths that
366 are much smaller, the ion microprobe will provide a greater sampling advantage such as
367 results found by Matta et al[9] who studied yellowfin sole biogeography and Hanson et al[36]
368 who studied salmon migration.

369 With micromilling methods on Pacific cod otoliths, some loss of information
370 probably occurred on the margin of the otolith, in material representing the last several years
371 of life. In many of the specimens the apparent amplitude of seasonal changes in $\delta^{18}O$ values
372 from micromilling was reduced near the otolith's margin compared to the ion microprobe
373 (Fig. 3). Indeed, one motivation for this study was to address concerns expressed by Kastelle
374 et al[11] and Hoie et al[8] that micromilling/IRMS can potentially result in signal attenuation of
375 $\delta^{18}O$ signal over the life history transect, thereby reducing distinctiveness in seasonal peaks
376 of $\delta^{18}O$ values used as a tool for fish age validation. Also, with micromilling it is difficult to
377 sample the ventral area of the thin sectioned otolith because in that region the growth zones
378 form a short radius curve and are less distinct; thus, we did not attempt this. However, the ion
379 microprobe method was able to include a second short transect of spots to analyze such areas.
380 In the regions sampled by both methods (i.e., not considering the second short transects in the
381 ventral region, shown by a different symbol in Fig. 3), the number of peaks were the same
382 with the exception of individuals 426 and 778. Hence, in the regions sampled by both
383 methods, the cyclic nature of the seasonal temperature histories was preserved by the
384 micromilling/IRMS (Fig. 3). These points suggest that under certain conditions of a short-
385 lived species, relatively large otoliths, or when considering only the first three or four years,
386 micromilling/IRMS is suitable. In a similar study by Hanson et al[36] the conclusions were

387 very similar, and depending on the information needed (they were looking for one distinct
388 change in $\delta^{18}O$ values related to smoltification in salmon (*Salmo salar*), the use of
389 micromilling was supported.

390 The precision of $\delta^{18}O$ values measured using micromilling/IRMS was better than that
391 from an ion microprobe, however sample mass requirements for IRMS are much greater
392 (>10,000 times). In this study, with micromilling and conventional IRMS, we achieved 95%
393 confidence intervals in the range of 0.1‰ from otolith aragonite sample masses as low as
394 ~30 μg. This precision does not necessarily ameliorate problems related to fish that are long-
395 lived or have small otoliths, which prevents adequate spatial or temporal resolution (i.e.,
396 seasonal zones are too narrow) to track migratory and thermal habitat behavior. For instance,
397 Matta et al[9] was able to acquire nearly biweekly $\delta^{18}O$ measurements with the ion microprobe
398 method during the first several years of life for yellowfin sole otoliths, but after a decade of
399 life fewer than three spots per growth year. In this instance micromilling/IRMS might at best
400 be able to obtain a single sample per year near the margin, and might still integrate material
401 from different years obscuring the annual signal in $\delta^{18}O$ values. The quality and structure of
402 the otolith can affect the precision of the ion microprobe measurements. For example, in
403 specimen 454 prior to the first peak the $\delta^{18}O$ values had an apparent scatter, and in the
404 respective part of the otolith sampled there was notable porosity. Theoretically, this porosity
405 could have caused the scatter of $\delta^{18}O$ values, possibly a loss of precision, and potentially a
406 signal loss (Fig. 3). We did not perform any tests to confirm the relationship between scatter
407 and the porosity. To avoid this issue care must be taken to not sample these areas of the
408 otolith with an ion microprobe. Fortunately, in the case of specimen 454, the porosity was
409 early in the transect, so it did not influence the interpretation of the results.

While the two methods produced a similar number of seasonal cycles, the average $\delta^{18}O$ values often differed, with SIMS $\delta^{18}O$ values being generally lower, except when $\delta^{18}O$ values peaked in the translucent (i.e., winter) zones (Fig. 3). In comparing $\delta^{18}O$ values sampled by micromilling/IRMS and the SIMS, there was a positive linear relationship whose slope is 0.477 and intercept is 0.482. The slope is less than 1 because of the larger range of intra-band variability in SIMS $\delta^{18}O$ data. However, this difference from a slope of 1 would exist even if there was no offset. One possible reason for the average observed offset of 0.53‰ could be if any water (incorporated in the otolith's aragonite crystal structure) was analyzed by the ion microprobe lower $\delta^{18}O$ values would be expected. A second possible reason for the offset between the two methods could relate to the presence of protein that is incorporated at a greater rate during warmer high growth seasons (opaque regions) than during colder season (translucent regions).[17-18] This protein contains hydroxyl groups (OH) which have lower $\delta^{18}O$; this may bias the ion microprobe results, because both the aragonite and protein contribute to the measured $\delta^{18}O$ value. Conversely, the acid digestion used in conventional IRMS does not react with the protein to form CO_2 gas. This eliminates the protein's low $\delta^{18}O$ from the IRMS. During the ion microprobe analysis we measured $^{16}O^{1}H$ in addition to ^{16}O and ^{18}O and found a general inverse relationship between values of $\delta^{18}O$ and $^{16}O^{1}H$ (Fig. 5). Therefore, the $\delta^{18}O$ peaks (expected to be in association with translucent zones and slow winter growth with proportionally less protein) corresponded to lower $^{16}O^{1}H$ values. Within the $\delta^{18}O$ troughs the corresponding $^{16}O^{1}H$ values were high and likely represent a period of time with faster summer growth (opaque zones), more intensive feeding, and hence where proportionally more protein matrix is deposited.[17-18] The 0.53‰ offset between IRMS and ion microprobe seen in this study is within the range of observed offsets observed by Orland et al[37], suggesting that organic matter or water within the

carbonate is being ionized during ion microprobe analysis. Matta et al[9] observed a ~1‰ offset when comparing ion microprobe analyses of $\delta^{18}O$ in roasted and unroasted otoliths.

5 CONCLUSIONS

Our objectives for this study were met. First, we determined that the $\delta^{18}O$ seasonal patterns (life-history signatures) derived from the two different sampling and mass spectrometry techniques were similar, especially when the growth zones are not extremely compact on the margin of the otolith. Second, we determined that under appropriate situations (i.e. large otoliths and short-lived fish) micromilling/IRMS can provide adequate resolution for fish age validation studies. However, the ion microprobe method is the only option for special situations, such as with smaller otoliths, longer lived specimens, or when greater temporal resolution is required. Third, both methods displayed life-history information on the depth and migration history of Pacific cod.

ACKNOWLEDGEMENTS

National Oceanic and Atmospheric Administration (NOAA), National Marine Fisheries Service, supported this research for which we are grateful. We thank Delsa Anderl of NOAA, National Marine Fisheries Service, for assistance with interpreting the Pacific cod otolith microstructure. Otolith samples and specimen data for this study were provided by Dan Nichol of NOAA, National Marine Fisheries Service, for which we are grateful. Thanks to Andy Whitehouse and Jim Murphy of NOAA, National Marine Fisheries Service, for thoughtful reviews of early manuscript drafts. At UW-Madison, we thank Noriko Kita and Jim Kern for assistance with SIMS analysis, John Fournelle for assistance with SEM imaging and Brian Hess for sample preparation. WiscSIMS is supported by National Science Foundation (EAR-1355590, 1658823) and the University of Wisconsin - Madison. Reference

to trade names does not imply endorsement by the NOAA, National Marine Fisheries Service. The findings and conclusions in the paper are those of the authors and do not necessarily represent the views of NOAA, National Marine Fisheries Service.

REFERENCES

1. Grossman EL, Ku TL. Oxygen and carbon isotope fractionation in biogenic aragonite: Temperature effects. *Chem Geol*. 1986;59:59-74. http://doi.org/10.1016/0168-9622(86)90057-6
2. Culleton BJ, Kennett DJ, Jones TL. Oxygen isotope seasonality in a temperate estuarine shell midden: a case study from CA-ALA-17 on the San Francisco Bay, California. *J Archaeol Sci*. 2009;36:1354-1363. doi:10.1016/j.jas.2009.01.021
3. Nielsen JK, Nielsen JK. Geoducks (*Panopea abrupta*) as isotopic bioarchives of seasonality in the climate of British Columbia. *Ecol Res*. 2009;24(5):987-995. doi:10.1007/s11284-008-0571-4
4. Lopez Correa M, Montagna P, Vendrell-Simon B, McCulloch M, Taviani M. Stable isotopes ($\delta^{18}O$ and $\delta^{13}C$), trace and minor element compositions of recent scleractinians and last glacial bivalves at the Santa Maria di Leuca deep-water coral province, Ionian Sea. *Deep-Sea Res. Pt II: Top. Stud. in Oceanogr.* 2010;57(5-6):471-486. doi:10.1016/j.dsr2/2009.08.016
5. Linzmeier BJ, Kozdon R, Peters SE, Valley JW. Oxygen Isotope Variability within Nautilus Shell Growth Bands. *PLoS ONE*. 2016;11(4): e0153890. https://doi.org/10.1371/journal.pone.0153890
6. Weidman CR, Millner R. High-resolution stable isotope records from North Atlantic cod. *Fish Res*. 2000;46(1-3):327-342.

480 7. Hoie H, Andersson C, Folkvord A, Karlsen, O. Precision and accuracy of stable isotope
481 signals in otoliths of pen-reared cod (*Gadus morhua*) when sampled with a high-
482 resolution micromill. *Mar Biol*. 2004;144:1039-1049.
483 8. Hoie H, Otterlei E, Folkvord A. Temperature-dependent fractionation of stable oxygen
484 isotopes in otoliths of juvenile cod (*Gadus morhua* L.). *ICES J Mar Sci*. 2004;61:243-
485 251.
486 9. Matta ME, Orland IJ, Ushikubo T, Helser TE, Black BA, Valley JW. Otolith oxygen
487 isotopes measured by high-precision secondary ion mass spectrometry reflect life history
488 of a yellowfin sole (*Limanda aspera*). *Rapid Commun Mass Spectrom*. 2013;27:691-699.
489 10. Helser T, Kastelle C, Crowell A, et al. A 200-year archaeozoological record of Pacific
490 cod (*Gadus macrocephalus*) life history as revealed through ion microprobe oxygen
491 isotope ratios in otoliths. *J Archaeol Sci Rep*. Early on line, Accessed March 13, 2018.
492 doi.org/10.1016/j.jasrep.2017.06.037.
493 11. Kastelle CR, Helser TE, McKay JL, et al. Age validation of Pacific cod (*Gadus*
494 *macrocephalus*) using high-resolution stable oxygen isotope ($\delta^{18}O$) chronologies in
495 otoliths. *Fish Res*. 2017;185:43-53.
496 12. Kalish JM. Oxygen and Carbon Stable Isotopes in the Otoliths of Wild and Laboratory-
497 Reared Australian Salmon (*Arripis trutta*). *Mar Biol*. 1991;110:37-47.
498 13. Thorrold SR, Campana SE, Jones CM, Swart PK. Factors determining $\delta^{13}C$ and $\delta^{18}O$
499 fractionation in aragonitic otoliths of marine fish. *Geochim Cosmochim Acta*.
500 1997;61:2909-2919.
501 14. Hoie H, Folkvord A. Estimating the timing of growth rings in Atlantic cod otoliths using
502 stable oxygen isotopes. *J Fish Biol*. 2006;68:826-837.

15. Darnaude AM, Sturrock A, Trueman CN, Mouillot D, Campana SE, Hunter E, EIMF. Listening In on the Past, What Can Otolith $\delta^{18}O$ Values Really Tell Us about the Environmental History of Fishes? *PLoS ONE*. 2014;9(10): e108539. https://doi.org/10.1371/journal.pone.0108539

16. Matta ME, Kimura DK. Age determination manual of the Alaska Fisheries Science Center Age and Growth Program. Professional Paper. NMFS 13. NOAA, National Marine Fisheries Service, Seattle, Washington. 2012.

17. Degens ET, Deuser WG, Haedrich RL. Molecular Structure and Composition of Fish Otoliths. *Mar Biol*. 1969;2:105-113.

18. Wright PJ, Panfili J, Morales-Nin B, Geffen AJ. Otolilths. In: Panfili J, de Pontual H, Troadec H, Wright JP, eds. *Manual of Fish Sclerochronology*. Brest, France: Ifremer-IRD coedition: 2002:31-57.

19. Weidel BC, Ushikubo T, Carpenter SR, et al. Diary of a bluegill (*Lepomis macrochirus*): daily $\delta^{13}C$ and $\delta^{18}O$ records in otoliths by ion microprobe. *Can J Fish Aquat Sci*. 2007;64:1641-1645.

20. Kozdon R, Ushikubo T, Kita NT, Spicuzza M, Valley JW. Intratest oxygen isotope variability in the planktonic foraminifer N. pachyderma: Real vs. apparent vital effects by ion microprobe. *Chem Geol*. 2009;258:327-337.

21. Valley JW, Kita NT. In Situ Oxygen Isotope Geochemistry By Ion Microprobe. In: Fayek M, ed. *Secondary Ion Mass Spectrometry in the Earth Sciences: Gleaning the Big Picture from a Small Spot*. Toronto Ontario, CA: Mineralogical Association of Canada, Short Course Series volume 41;2009:19-63.

22. Nichol DG, Chilton EA. Recuperation and behaviour of Pacific cod after barotrauma. *ICES J Mar Sci*. 2006;63:83-94.

527 23. Nichol DG, Kotwicki S, Zimmermann M. Diel vertical migration of adult Pacific cod
528 Gadus macrocephalus in Alaska. *J Fish Biol*. 2013;83:170-189.
529 24. Gao Y, Crowley S, Conrad R, Dettman DL. Effects of organic solvents on stable isotopic
530 composition of otolith and abiogenic aragonite. *Palaeogeogr Palaeoclimatol Palaeoecol*.
531 2015;440:487-495.
532 25. Johnston C, Anderl DM. Pacific cod (*Gadus macrocephalus*). In: Matta ME, Kimura DK,
533 eds. *Age Determination Manual of the Alaska Fisheries Science Center Age and Growth*
534 *Program.* Professional Paper NMFS 13. Seattle, WA. NOAA, National Marine Fisheries
535 Service; 2012:25-30.
536 26. Kim ST, Mucci A, Taylor BE. Phosphoric acid fractionation factors for calcite and
537 aragonite between 25 and 75 degrees C, Revisited. *Chem Geol*. 2007;246;135-146.
538 27. Kita NT, Ushikubo T, Fu B, Valley JW. High precision SIMS oxygen isotope analysis
539 and the effect of sample topography. *Chem Geol*. 2009;264:43-57.
540 28. Orland IJ, Bar-Matthews M, Kita NT, Ayalon A, Matthews A, Valley JW. Climate
541 deterioration in the Eastern Mediterranean as revealed by ion microprobe analysis of a
542 speleothem that grew from 2.2 to 0.9 ka in Soreq Cave, Israel. *Quatern Res*. 2009;71:27-
543 35.
544 29. Jones JB, Campana, SE. Stable oxygen isotope reconstruction of ambient temperature
545 during the collapse of a cod (*Gadus morhua*) fishery. *Ecol Appl*. 2009;19:1500-1514.
546 30. Laurel BJ, Stoner AW, Ryer CH, Hurst TP, Abookire AA. Comparative habitat
547 associations in juvenile Pacific cod and other gadids using seines, baited cameras and
548 laboratory techniques. *J Exp Mar Biol and Ecol*. 2007;351;42-55.

549 31. Stoner AW, Laurel BJ, Hurst TP. Using a baited camera to assess relative abundance of
550 juvenile Pacific cod: Field and laboratory trials. *J Exp Mar Biol and Ecol*. 2008;354:202-
551 211.
552 32. Laurel BJ, Ryer CH, Knoth B, Stoner AW. Temporal and ontogenetic shifts in habitat use
553 of juvenile Pacific cod (*Gadus macrocephalus*). *J Exp Mar Biol and Ecol*. 2009;377:28-
554 35.
555 33. Nichol DG, Honkalehto T, Thompson GG. Proximity of Pacific cod to the sea floor:
556 Using archival tags to estimate fish availability to research bottom trawls. *Fish Res*.
557 2007;86:129-135.
558 34. Stark JW. Geographic and seasonal variations in maturation and growth of female Pacific
559 cod (*Gadus macrocephalus*) in the Gulf of Alaska and Bering Sea. *Fish Bull*.
560 2007;105:396-407.
561 35. Harwood J, Aplin AC, Fialips CI, et al. Quartz Cementation History of Sandstones
562 Revealed by High-Resolution Sims Oxygen Isotope Analysis. *J Sediment Res*.
563 2013;83:522-530.
564 36. Hanson NN, Wurster CM, EIMF, Todd CD. Comparison of secondary ion mass
565 spectrometry and micromilling/continuous flow isotope ratio mass spectrometry
566 techniques used to acquire intra-otolith $\delta^{18}O$ values of wild Atlantic salmon (*Salmo*
567 *salar*). *Rapid Commun Mass Spectrom*. 2010;24:2491-2498.
568 37. Orland IJ, Kozdon R, Linzmeier B, et al. Enhancing the accuracy of carbonate $\delta^{18}O$ and
569 $\delta^{13}C$ measurements by SIMS. American Geophysical Union, Fall Meeting, December 18,
570 2015. Presentation PP52B-03.
571 https://agu.confex.com/agu/fm15/meetingapp.cgi/Paper/67486. Accessed April 6, 2018.

Table 1.

Biological information, sampling results, and $\delta^{18}O$ measurement results for the Pacific cod (*Gadus macrocephalus*). The number of SIMS points refers to ion microprobe sampling spots as compared to the milled track samples in the micromilling.

Sample ID	# growth zones on SIMS	# growth zones milled	Number of SIMS points (compared [a])	SIMS transect length (mm)[b]	SIMS, samples per mm	# milled tracks (# compared [a])	Total length milled (mm)[b]	Milling, tracks per mm	SIMS $\delta^{18}O$ average (‰ VPDB)	1 SD	IRMS $\delta^{18}O$ average (‰ VPDB)	1 SD
253	5	5	52 (49)	2.575	20.194	33 (31)	1.810	18.232	-0.02	0.68	0.78	0.39
426	5	5	61 (61)	2.815	21.670	33 (26)	2.468	13.371	-0.77	1.2	0.32	0.44
454	5	5	77 (75)	2.584	29.799	42 (40)	1.793	22.424	0.19	0.79	0.54	0.31
693	5	4	90 (90)	1.947	46.225	35 (33)	1.665	21.021	-0.65	0.93	0.09	0.69
778	6	6	82 (82)	2.091	39.216	44 (39)	2.127	20.686	0.21	1.08	0.18	0.90
812	5	5	90 (87)	1.438	62.587	38 (38)	1.642	23.143	-0.07	1.64	0.14	1.14

[a] Number of points compared is reduced from the total number due to occasional problems with mass spectrometry.

[b] Ion microprobe transect length and total length milled are comparable features in the two methods. The length milled is the sum of track widths.

[c] In per mil VPDB.

Figure Captions

Figure 1: Map of tagging and recovery locations of Pacific cod (*Gadus macrocephalus*).

Figure 2: Image of otolith transverse thin section from Pacific cod (*Gadus macrocephalus*) specimen 812. The distal region of micromilling and transect of ion probe spot samples are enlarged. Note, this was the only specimen out of 6 where the ion microprobe transect was contiguous. In all other specimens a second short transect of ion probe spots was made in the ventral tip (otolith's lower tip in the image).

Figure 3: Results of $\delta^{18}O$ (‰ VPDB) measurements by two methods, SIMS in the first main transect (triangles) or in a second short transect (squares) and micromilling with IRMS (circles) in otoliths from Pacific cod (*Gadus macrocephalus*). Error bars are 95% confidence intervals.

Figure 4: Average values of $\delta^{18}O$ (‰ VPDB) from micromilling and IRMS vs. average values $\delta^{18}O$ (‰ VPDB) from the ion microprobe (SIMS), for the three different sections in each specimen Pacific cod (*Gadus macrocephalus*). The description of the sections are described in the text. The solid line is a linear fit to all points, and the equation and correlation are provided. The dashed line is 1:1 (45º). The slope is less than 1 due to the larger range of intra-band variability in SIMS $\delta^{18}O$ data. Note, this difference from 1 would exist even if there was not an average offset of 0.53‰.

Figure 5: Plots of $^{16}O^{1}H/^{16}O$ values vs. $\delta^{18}O$ (‰ VPDB) values measured by SIMS in Pacific cod (*Gadus macrocephalus*) specimen 812. A) Variations in values of $\delta^{18}O$ (‰ VPDB) (triangles) and $^{16}O^{1}H/^{16}O$ ratios (open circles) across the otolith and B) the relationship between values of $\delta^{18}O$ and $^{16}O^{1}H/^{16}O$ (‰ VPDB) ratios.

Figure 1.

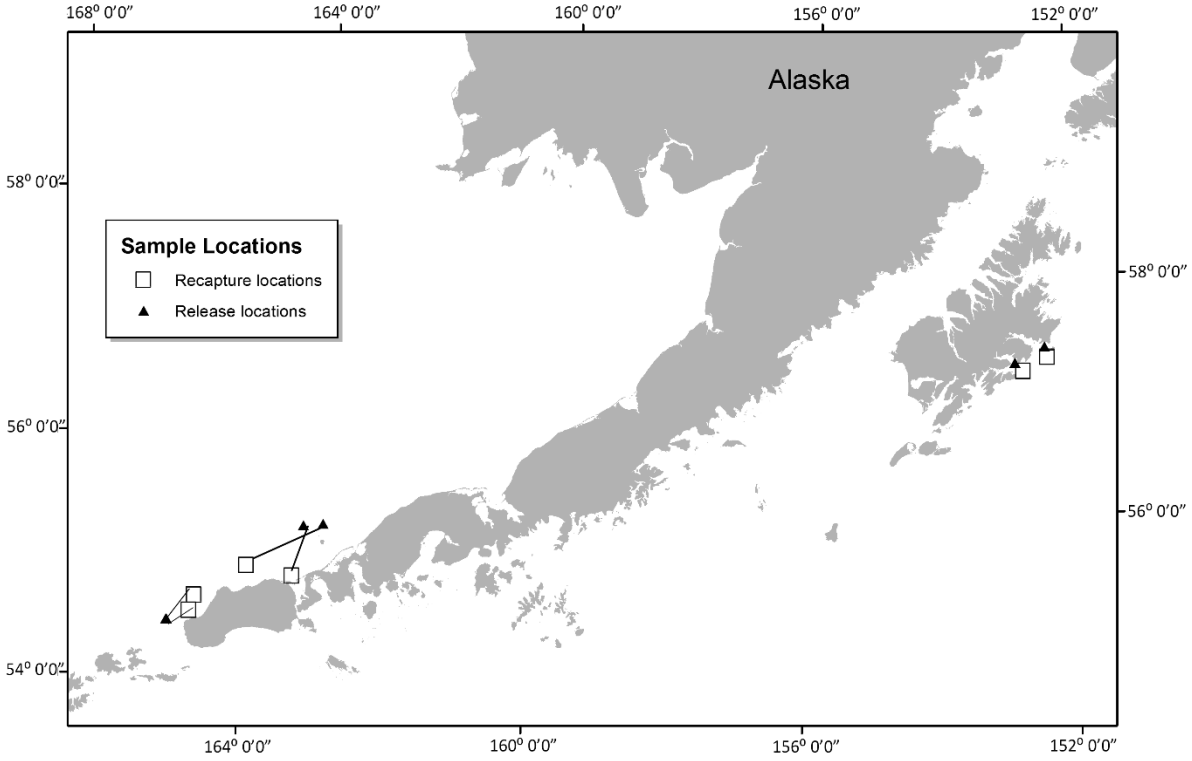
168° 0′0″
164° 0′0″
160° 0′0″
156° 0′0″
152° 0′0″
Alaska
58° 0′0″
56° 0′0″
54° 0′0″
Sample Locations
Recapture locations
Release locations
164° 0′0″
160° 0′0″
156° 0′0″
152° 0′0″

Figure 2

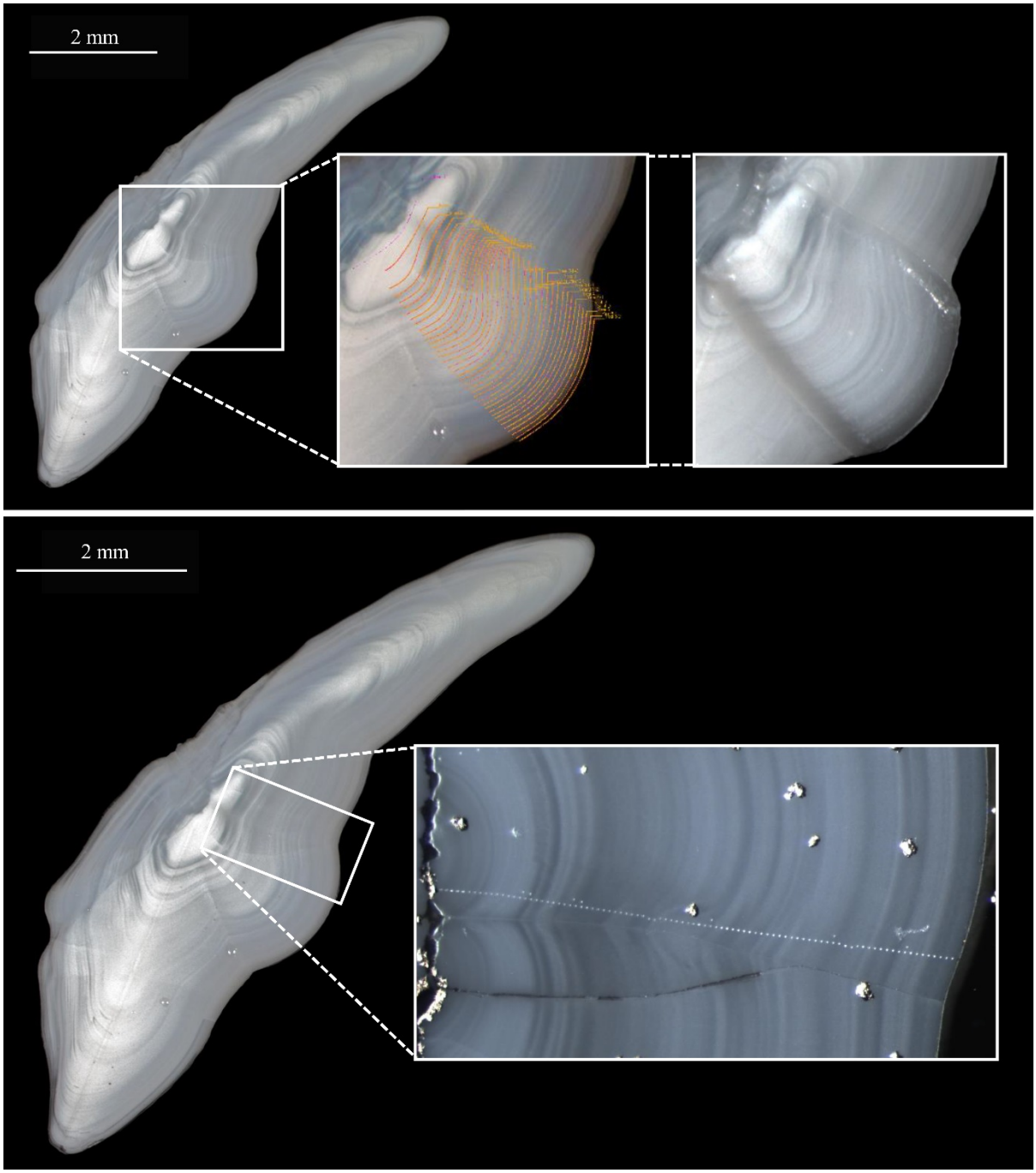

Figure 3

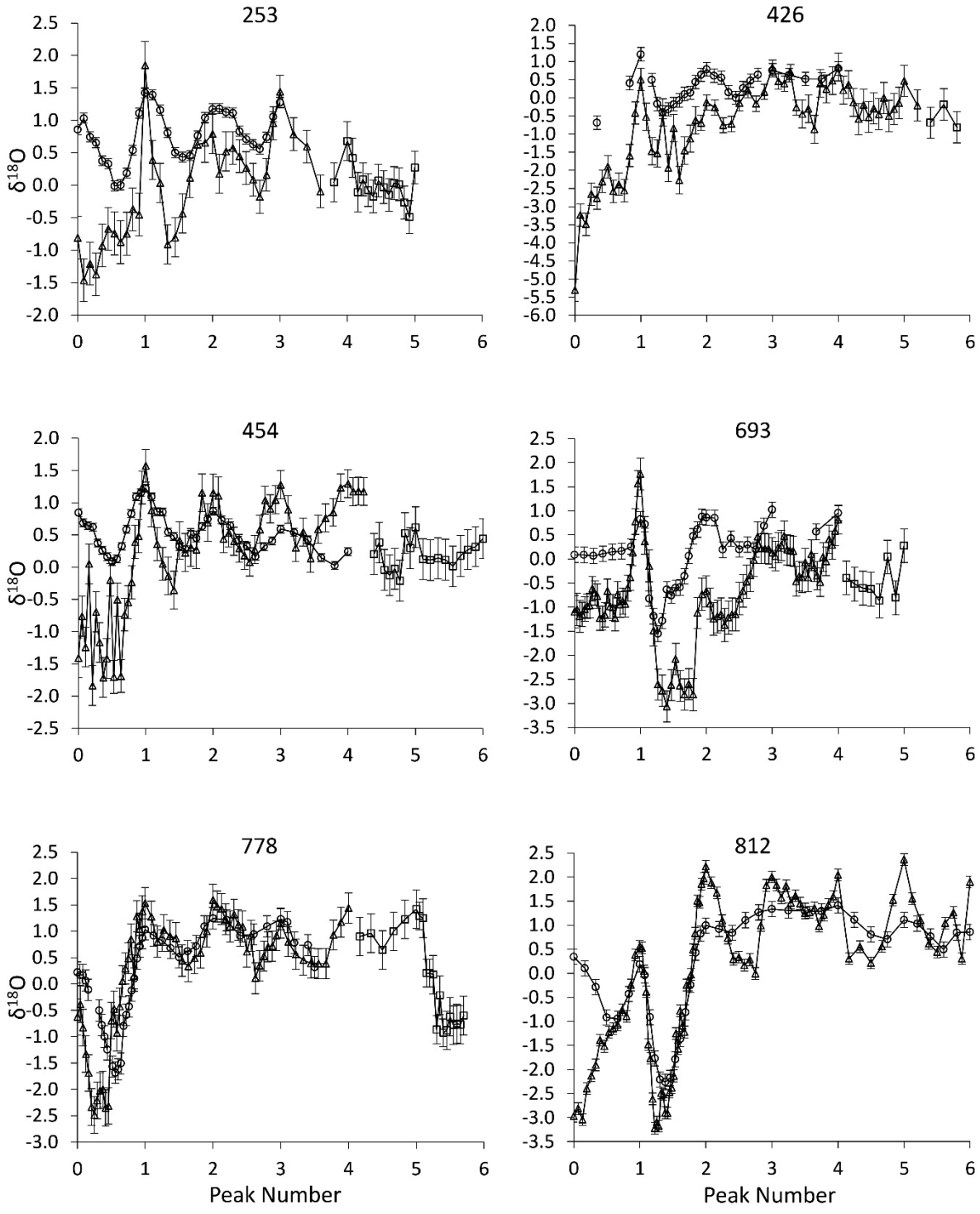

Figure 4.

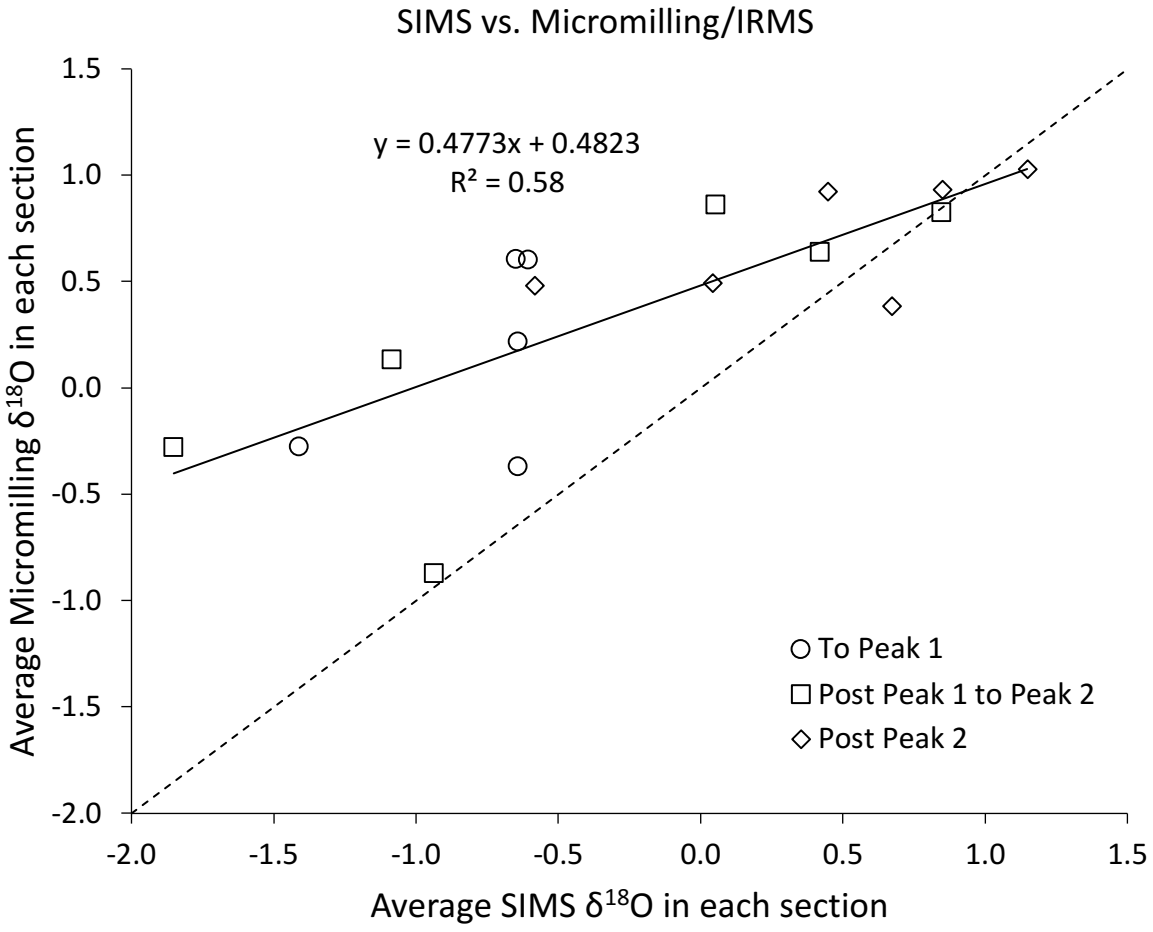
SIMS vs. Micromilling/IRMS
y = 0.4773x + 0.4823
R² = 0.58
Average Micromilling δ18O in each section
Average SIMS δ18O in each section
To Peak 1
Post Peak 1 to Peak 2
Post Peak 2
1.5
1.0
0.5
0.0
-0.5
-1.0
-1.5
-2.0
-2.0
-1.5
-1.0
-0.5
0.0
0.5
1.0
1.5

Figure 5

A

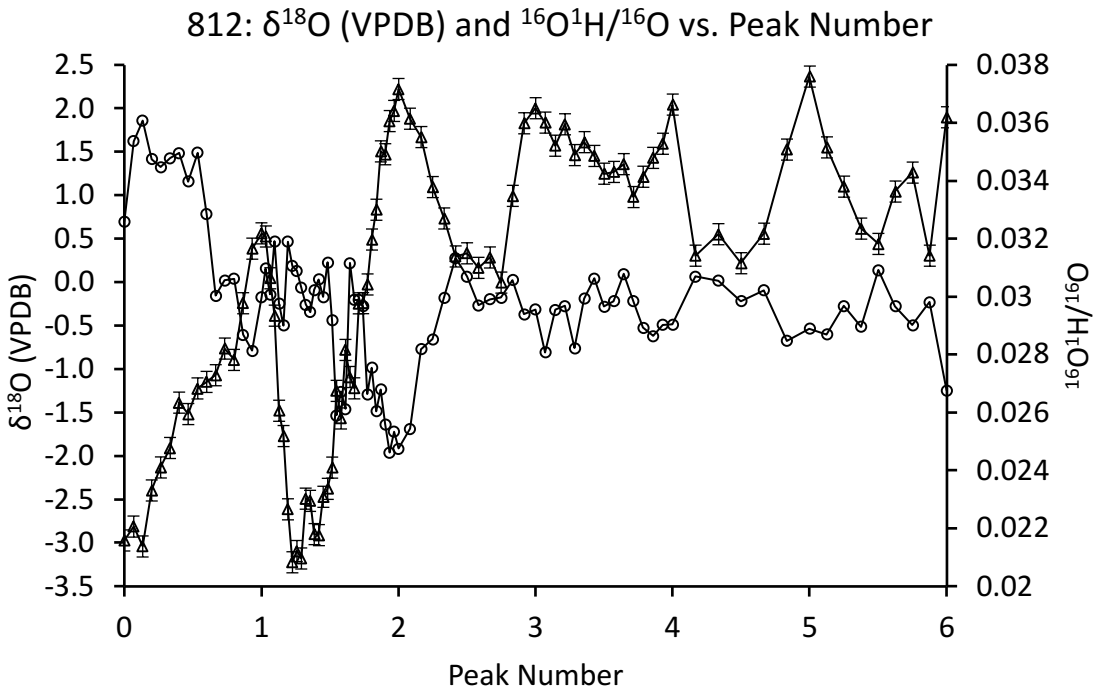
812: δ18O (VPDB) and 16O1H/16O vs. Peak Number
δ18O (VPDB)
16O1H/16O
Peak Number
2.5
2.0
1.5
1.0
0.5
0.0
-0.5
-1.0
-1.5
-2.0
-2.5
-3.0
-3.5
0.038
0.036
0.034
0.032
0.03
0.028
0.026
0.024
0.022
0.02
0
1
2
3
4
5
6

Figure 5

B

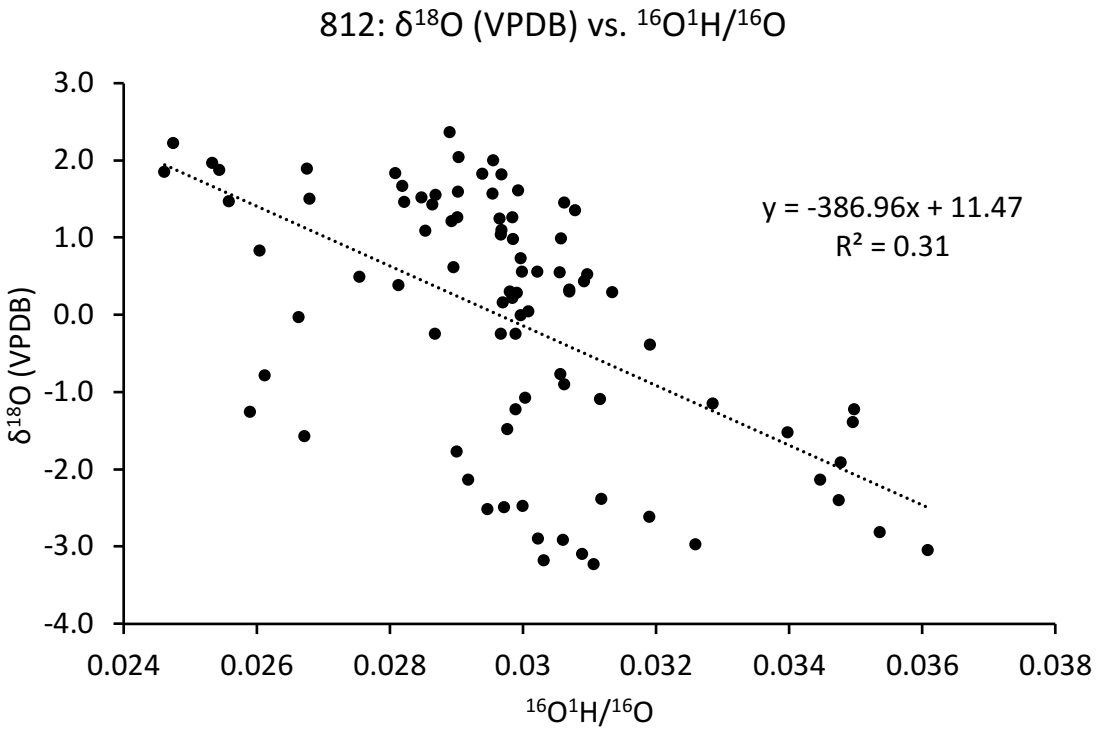
812: δ18O (VPDB) vs. 16O1H/16O
y = -386.96x + 11.47
R² = 0.31
δ18O (VPDB)
16O1H/16O
3.0
2.0
1.0
0.0
-1.0
-2.0
-3.0
-4.0
0.024
0.026
0.028
0.03
0.032
0.034
0.036
0.038